Effects of Silver Nanoparticles on the Dynamic Crystallization and Physical Properties of Syndiotactic Polypropylene

Dong Wook Chae,[1] Kwang Bo Shim,[2] Byoung Chul Kim[1]

[1]*Division of Applied Chemical and Bio Engineering, Hanyang University, 17 Haengdang, Seongdong, Seoul 133-791, Korea*
[2]*Department of Ceramic Engineering, CPRC, Hanyang University, 17 Haengdang, Seongdong, Seoul 133-791, Korea*

Received 14 April 2007; accepted 8 March 2008
DOI 10.1002/app.28340
Published online 20 May 2008 in Wiley InterScience (www.interscience.wiley.com).

ABSTRACT: The effects of silver (Ag) nanoparticles on the physical properties of syndiotactic PP (sPP) were investigated concentrating on the isothermal melt crystallization behavior under shear. sPP with 5 wt % Ag nanoparticles presented higher crystallization temperature (T_c) and heat of crystallization (ΔH_c) than pure sPP. At 90°C, the Ag nanoparticles had little effect on the induction time of crystallization but a little increased the half-time ($t_{1/2}$) for the crystallization. At 100°C, however, the induction time was decreased with increasing the Ag content and the $t_{1/2}$ was decreased up to the Ag content of 0.5 wt %. DSC melting endotherms exhibited double melting peaks when crystallized at 90°C under shear but a single melting peak when crystallized at 100°C. The WAXD patterns exhibited that the presence of Ag nanoparticles did not produce any change in the crystal structure of sPP. The tensile strength of sPP is little changed up to the Ag content of 0.1 wt % but it was decreased with further addition. In addition, the introduction of less than 0.1 wt % Ag increased the elongation at break, but further addition decreased it abruptly. © 2008 Wiley Periodicals, Inc. J Appl Polym Sci 109: 2942–2947, 2008

Key words: syndiotactic polypropylene; silver nanoparticles; crystallization; shear; physical properties

INTRODUCTION

Organic–inorganic hybrids are widely used because the functionalities of inorganic materials can be combined with the organic polymer.[1,2] Recently, thanks to the feasibility of the preparation of nanoscale filler its application to polymer matrix attracts great interest. The nanocomposites exhibit the outstanding advantages derived from nanoscale phenomena such as excellent processing properties, lower thermal expansion coefficient, higher swelling resistance, and gas permeability even at very low loading level.[3–7]

The presence of nanoparticles can modify the crystallization and melting behavior of polymeric materials. Further, the final properties of the inorganic filled polymer composites are seriously dependent on the thermal or shear histories which are imposed under processing because they affect the resultant morphology of the composites.[8] Thus, it is of great technological importance in all fabrication processes such as injection molding, extrusion, fiber spinning, and film blowing, to understand the effects of shear on the nucleation and crystallization processes because this offers a critical clue to optimize processing conditions and to improve the performance of final products.[9–12] In case of nanoscale particle filled polymeric systems, their characteristic features are not well understood. This is attributed to the unusually large specific surface area of the nanoparticles that strongly affects crystallization behavior and macroscopic properties of the base polymer, even at very low loading level. However, only a limited number of research works has been carried out on the crystallization behavior of the nanocomposites under shear which is related to the engineering application.

Syndiotactic PP (sPP) is claimed to have higher levels of transparency, heat resistance, and low temperature toughness in comparison with isotactic PP (iPP).[13] The stereostructure of a polymer chain often significantly affects the physical properties of the polymer together with molecular weight and chemical composition. Recently, many research on the nanocomposites based on the sPP are carried out.[14–17] Inclusion of Ag nanoparticles is expected to impart bacterial killing and electromagnetic shielding properties to sPP. In this study, sPP/Ag nanocomposites were prepared by melt mixing and the effect of Ag nanoparticles on the physical properties were discussed focusing on the isothermal melt crystallization behavior under shear and resultant morphology.

Correspondence to: B. C. Kim (bckim@hanyang.ac.kr).

EXPERIMENTAL

Materials

Syndiotactic polypropylene (sPP: number average molecular weight = 17,400), were purchased from Aldrichs. In addition, a round-shaped silver (Ag) nanoparticle (average size = 46.2 nm, standard deviation = 6.45) was supplied by NP-Tech (Korea). The sPP was vacuum dried at 60°C for 24 h before melt mixing with Ag nanoparticles. The sPP and Ag nanoparticles were premixed by tumbling and then melt-compounded in an internal mixer (Haake Rheomix 600) for 5 min at 190°C at a rotor speed of 60 rpm. The loading levels (X) of the nanocomposites were 0.01, 0.1, 0.5, 1, and 5 wt %, and they were coded sPP-X.

Dynamic crystallization and physical properties

Field emission scanning electron microscopic (FESEM; JEOL, JSM-6340F) experiment was carried out on the surface of the nanocomposites in a sheet formed by compression molding.

The rheological properties of the nanocomposites were investigated by a rotational rheometer (Advanced Rheometric Expansion System (ARES); Rheometric Scientific, Inc.) in an oscillatory mode. Parallel plate geometry with a diameter of 25 mm was employed. The plate gap and strain level were 1 mm and 5%, respectively. The specimen was melted at 150°C between plates and then kept for 5 min at the temperature in nitrogen atmosphere to remove residual stress. For time sweep measurement the given shear rates of 1 and 5 rad/s were applied immediately after quenching from 150°C to the predetermined crystallization temperatures, 90 and 100°C.

Wide angle X-ray diffraction (WAXD) experiments were carried out by Rigaku Denki (D/MAX-2000) with Nickel filtered CuKα radiation of 40 kV and 100 mA. Scanning was carried out on the equator in the 2θ range from 5 to 80° at a scan speed of 5°/min.

Differential scanning calorimetry (DSC) measurement was carried out by DSC 2010 (TA Instruments, Dupont). The sPP/Ag nanocomposites were held at 150°C for 5 min to eliminate the effect of thermal history, and the cooling scan was obtained at the cooling rate of 10 K/min. The heating scan was also obtained for the specimen isothermally crystallized under shear at a heating rate of 10 K/min in nitrogen atmosphere.

Thermal gravimetric analysis (TGA) was carried out by SDT2960 (TA Instruments, Dupont). Samples were heated to 800°C at a heating rate of 10 K/min in a nitrogen atmosphere.

The mechanical properties of the samples were measured by Instron tensile tester model 4465 at room temperature using dog bone-shaped specimens (ASTM D638 Type V). The gauge length and crosshead speed were 25 mm and 10 mm/min, respectively. Average values of 10 measurements were taken as the data.

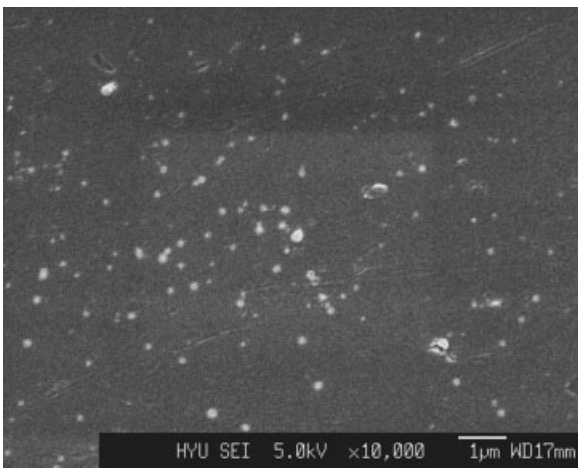

Figure 1 FESEM images of the surface of sPP-5 sheet.

RESULTS AND DISCUSSION

Figure 1 presents FESEM image of the surface of the sPP nanocomposite film with 5 wt % Ag. The Ag nanoparticles are dispersed uniformly in the sPP matrix although their small agglomerate is sparsely observed.

The cooling scan thermograms of as-prepared samples in Figure 2 show that sPP is a slowly crystallizing polymer. The introduction of Ag nanoparticles increases the crystallization temperature (T_c) and heat of crystallization (ΔH_c) with the loading level. When comparing the parameters of pure sPP to those of sPP-5, T_c and ΔH_c are increased from 57.9 to 70.2°C and from 23.1 to 27.2 J/g, respectively. This suggests that the Ag nanoparticles induce heterogeneous nucleation and increase the degree of crystallization. In addition, the crystallization peak becomes sharp with increasing the Ag content. This indicates that uniform size of crystal is formed by the presence of Ag nanoparticles.

Figure 3 exhibits TGA thermograms of sPP and sPP/Ag nanocomposites. Introducing the Ag nanoparticles increases the thermal stability of sPP with Ag content. When comparing the $T_{0.1}$ of the samples, the temperature required for 10% degradation, sPP-5 shows higher $T_{0.1}$ than sPP by 25°C. This is likely to be a result of the shielding effect of Ag through the physical association between the nanoparticles and the polymer chains, impeding the out-diffusion of volatile by-products generated during polymer degradation.[18,19] In addition, in the derivative TGA

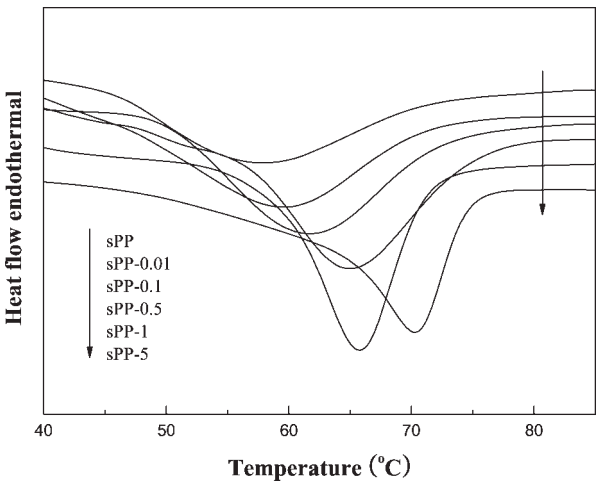

Figure 2 DSC cooling scan thermograms of as-prepared samples.

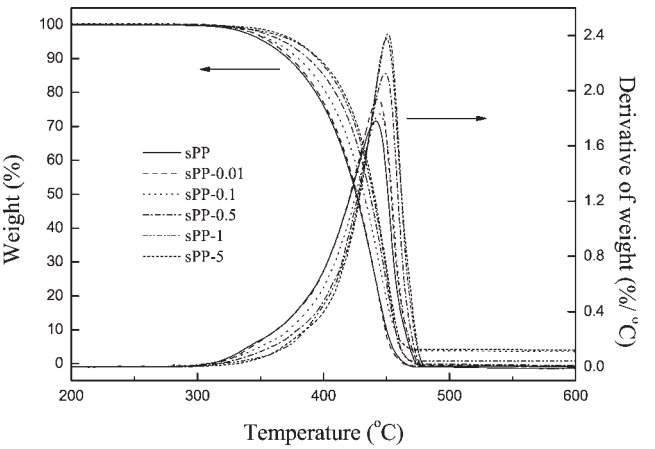

Figure 3 TGA thermograms of sPP and sPP/Ag nanocomposites.

curve, a temperature (T_{max}), where the highest weight reduction occurs, is also increased from 441.6 to 450.1°C with increasing the Ag content. It is worth noting that all samples display a single peak in the curve. This indicates that the Ag loading has little influence on the degradation step of sPP.

Figure 4 shows the variation of storage modulus (G′) with time for sPP and sPP/Ag nanocomposites at 1 and 5 rad/s at 90 and 100°C. In rheological prin-

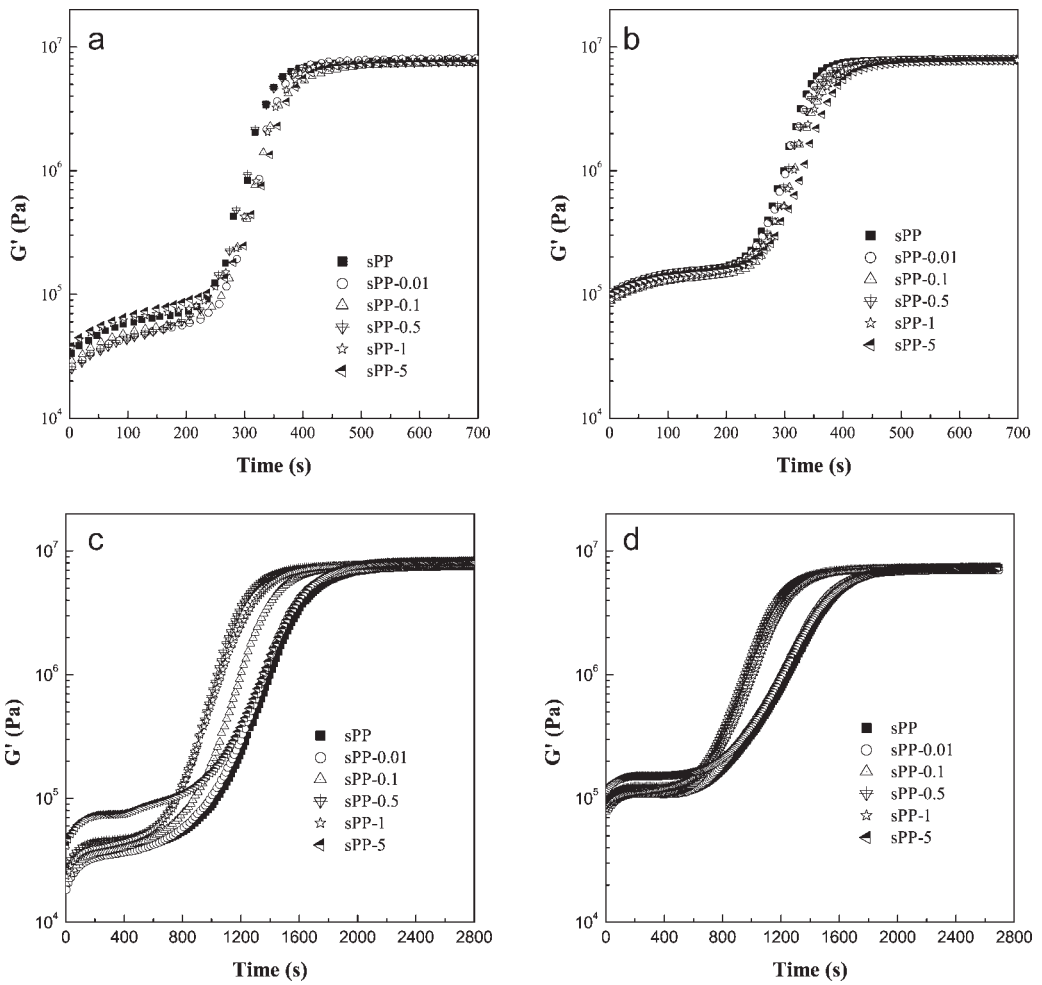

Figure 4 Variation of G′ with time at (a) 90°C and ω = 1 rad/s, at (b) 90°C and ω = 5 rad/s, at (c) 100°C and ω = 1 rad/s, and at (d) 100°C and ω = 5 rad/s.

TABLE I
Induction Time and Half Time of Crystallization ($t_{1/2}$) Data Determined from the G′ Versus Time Curves

Temperature and frequency	Sample	Induction time (s)	$t_{1/2}$ (s)
90°C, 1 rad/s	sPP	205	157
	sPP-0.01	204	156
	sPP-0.1	203	162
	sPP-0.5	197	158
	sPP-1	205	159
	sPP-5	198	176
90°C, 5 rad/s	sPP	192	143
	sPP-0.01	190	150
	sPP-0.1	194	167
	sPP-0.5	190	162
	sPP-1	197	169
	sPP-5	192	186
100°C, 1 rad/s	sPP	523	1101
	sPP-0.01	525	1052
	sPP-0.1	515	884
	sPP-0.5	437	784
	sPP-1	426	864
	sPP-5	425	1180
100°C, 5 rad/s	sPP	495	1021
	sPP-0.01	487	967
	sPP-0.1	430	774
	sPP-0.5	426	730
	sPP-1	413	812
	sPP-5	413	1075

ciple, the isothermal crystallization behavior under shear can be evaluated by tracking G′ with time at a given temperature. G′ increases monotonously with time at the early stage of experiment, which is referred to as an induction time for crystallization. Then an abrupt increase of G′ is followed in a minute due to the formation of crystallites.[20,21] With crystallite growth the homogeneous melt changes to the heterogeneous suspension and G′ is increased with time.[22] In the G′-time curve, the level-off of G′ is regarded as an equilibrium state. In general, time to reach the equilibrium is equivalent to the overall crystallization time. This G′ versus time data can be normalized to give a relative crystallinity function of time, from which the half-time for crystallization ($t_{1/2}$) is determined. The induction time and $t_{1/2}$ obtained from the plot are summarized in Table I. At the crystallization temperature of 90°C, the Ag nanoparticles have little effect on the induction time indicating that the nucleation activity is weak at a low crystallization temperature. However, at 100°C the induction time is decreased with increasing the Ag content. At relatively high crystallization temperature, less favorable conditions for nucleation, the role of the nanoparticle acting as a nucleating agent is more effective leading to a decreased induction time with increasing the Ag content. At 90°C the Ag nanoparticles a little increase the $t_{1/2}$ of sPP. On the other hand, the $t_{1/2}$ is decreased up to the Ag content of 0.5 wt % at 100°C. However, further introduction retards the crystallization with increasing the Ag content. This suggests that the Ag nanoparticles play a role in hindering the motion of polymer chain. The decelerated crystallization behavior with the Ag loading at 90°C is ascribed to a lower mobility of polymer chain than at 100°C. The rate of crystallization of polymers is determined from a concurrent nucleation and growth processes, with nucleation being the dominant factor with nearing melting temperature. At a high loading level, however, Ag nanoparticles remarkably retard the growth of crystallites leading to an increase of $t_{1/2}$. In addition, the promoting effect of shearing on the crystallization behavior is notably observed at 100°C. As well known the crystallization rate is greatly determined by uncoiling of the chains. Since the extent of disentanglement and orientation, which is the very rate determining step in the crystallization of polymers, is increased with shear rate shearing accelerates the crystallization. The initial value of G′ is increased with an applied frequency. In the early stages, just after being cooled to the crystallization temperature, the polymer is present in the melt state. At the start of the time-sweep measurements, the higher frequency exerts a higher torque. Thus, the initial value of G′ is higher at higher frequency.

According to the WAXD diffractograms of the above-mentioned samples in Figure 5, the characteristic crystalline peaks are present at the scattering angle, $2\theta = 12.0$, 16.0, 20.5, and 24.4, corresponding to the reflection planes of sPP at (200), (010), (111), and (400), respectively. In addition, the diffraction peaks at $2\theta = 37.9°$, 44.0°, 64.1°, and 77.2°, which get more prominent with increasing the Ag content, represent (111), (200), (220), and (311) planes of Ag, respectively. The WAXD patterns show that Ag nanoparticles do not produce any new diffraction peaks and peak shift indicating that there is no formation of new crystal structure in the interface. However, the intensity of crystalline peak associated with sPP is decreased abruptly at the Ag content as high as 5 wt % because of a great reduction of sPP amount on the surface of the nanocomposites. In addition, the shearing level and crystallization temperature have little effect on the crystal structure.

Figure 6 presents DSC thermograms of sPP and sPP/Ag nanocomposites isothermally crystallized at the same conditions as given in Figure 4. They exhibit a double melting behavior in the vicinity of 121 (T_{m1}) and 129°C (T_{m2}) when crystallized at 90°C. T_{m1} is attributed to the melting of primary crystallites formed at the isothermal temperature and T_{m2} corresponds to the melting of crystallites produced by melt-recrystallization.[23] On the contrary, the samples crystallized at 100°C give a single T_m at 126°C, resulting from the melting of primary crystallites.

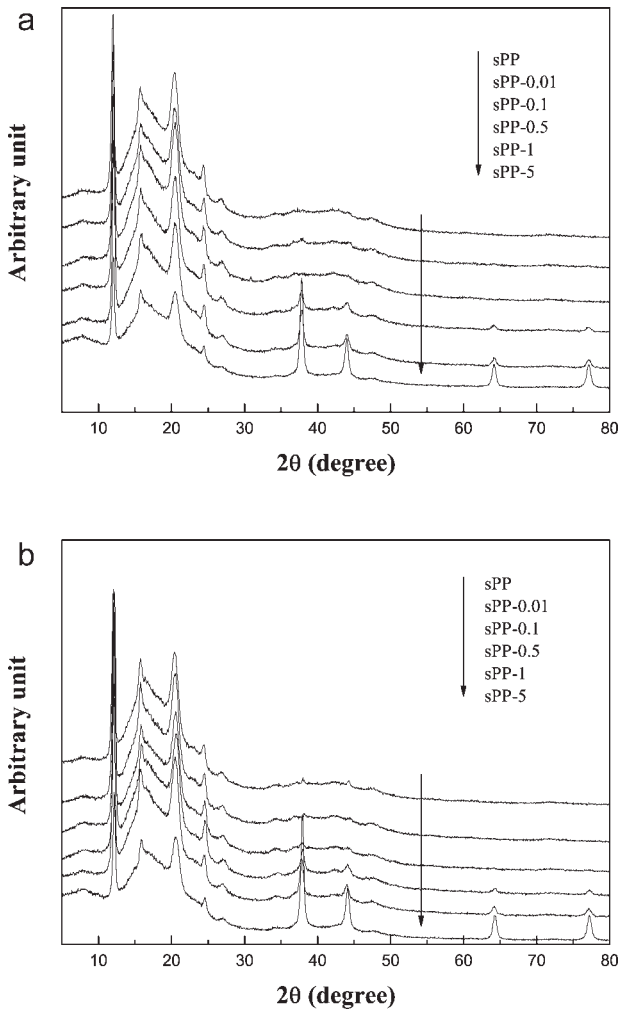

Figure 5 WAXD profiles of sPP and sPP/Ag nanocomposites crystallized at (a) 90°C and ω = 1 rad/s, and at (b) 100°C and ω = 5 rad/s.

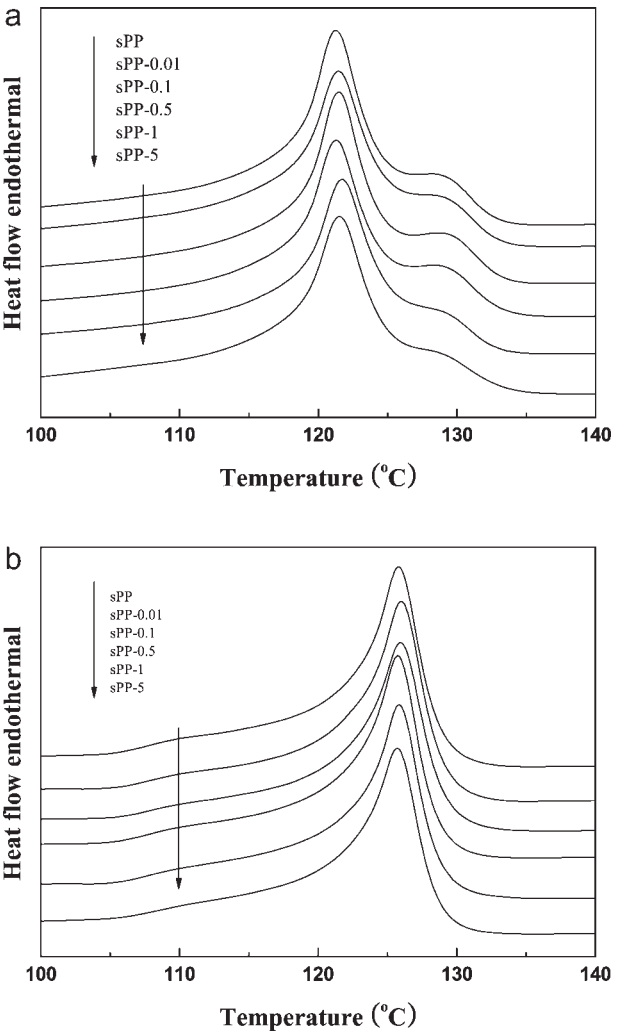

Figure 6 Heating scan thermograms of sPP and sPP/Ag nanocomposites crystallized at (a) 90°C and ω = 1 rad/s, and at (b) 100°C and ω = 5 rad/s.

The 5°C higher melting peak associated with the primary crystallites at 100°C than 90°C is indicative of the formation of larger crystallite because less nucleation site exists. In addition, the absence of the peak for the recrystallization at 100°C suggests that more stable crystallites are formed at the higher isothermal crystallization. Shearing level has little influence on the melting behavior of the nanocomposites, which agrees well with the WAXD data.

The stress–strain curves of sPP and sPP/Ag nanocomposites are shown in Figure 7. The samples exhibit a yield behavior and then the upturn to a high stress. The incorporation of Ag nanoparticles decreases the ductile properties of sPP. This indicates that the nanocomposites become brittle with increasing Ag content because of the stress concentration effect of the nanoparticles. Tensile strength is little changed up to the Ag content of 0.1 wt %, but further addition decreases it from 28.8 to 20.5 MPa with increasing the Ag content. An increased hetero-

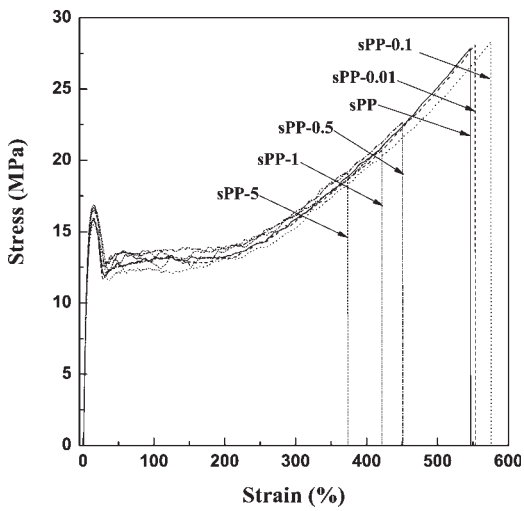

Figure 7 Stress–strain curve of sPP and sPP/Ag nanocomposites.

geneity in the sPP matrix with Ag content is more likely to introduce premature flaws, raising localized stress before fracture. Thus, the fracture resistance is decreased progressively with increasing the Ag content. The loading of less than 0.1 wt % Ag increases the elongation at break from 528.0 to 553.8%, but further addition decreases it abruptly. The Ag nanoparticles play a role in stopping crack growth at a low Ag content. However, at a high loading level, there exists some polymer chain entrapped by the Ag nanoparticles, which is immobilized and cannot deform as part of the matrix. This less deformable matrix results in a decrease of elongation at break. The significant reduction of elongation at break may also result in low toughnable properties.

CONCLUSIONS

This work focuses on the isothermal melt crystallization behavior under shear of sPP/Ag nanocomposites and their resultant morphology. The Ag nanoparticles promote the crystallization behavior leading to a high crystallization temperature and a short time to complete the crystallization. sPP needs a long processing time because sPP is a very slowly crystallizing polymer. Thus, the introduction of the Ag nanoparticles may be of great help to overcome the weak point of sPP in the processing. In addition, the Ag nanoparticles improve the thermal stability of sPP by showing a high degradation temperature with increasing the Ag content.

At an isothermal crystallization temperature of 90°C, Ag nanoparticles retard the crystallization a little. However, they promote the crystallization behavior up to 0.5 wt % loading at 100°C, but further addition increases the half-time for crystallization time with Ag content. This suggests that the Ag nanoparticles in the matrix not only act as a nucleating agent but also reduce the chain mobility. Polymer crystallization is determined from concurrent nucleation and growth processes. In other words, the competition between these two conflicting roles of the nanoparticles determines overall crystallization behavior of the composites. Thus, both roles should be in good harmony for favorable conditions of the crystallization.

References

1. Mitzi, D. B. Chem Mater 2001, 13, 3283.
2. Manias, E.; Touney, A.; Wu, L.; Strawhecker, K.; Lu, B.; Chung, T. C. Chem Mater 2001, 13, 3516.
3. Sun, T.; Garces, M. Adv Mater 2002, 14, 128.
4. Messersmith, P. B.; Giannelis, E. P. Chem Mater 1994, 6, 1719.
5. Messersmith, P. B.; Giannelis, E. P. J Polym Sci Part A: Polym Chem 1995, 33, 1047.
6. Kim, T. H.; Jang, L. W.; Lee, D. C.; Choi, H. J.; Jhon, M. S. Macromol Rapid Commun 2002, 23, 191.
7. Yeh, J. M.; Liou, S. J.; Lai, C. Y.; Wu, P. C. Chem Mater 2002, 14, 154.
8. Lee, O.; Kamal, M. R. Polym Eng Sci 1999, 39, 236.
9. Eder, G.; Janeschitz-Kriegl, H.; Liedauer, S. Prog Polym Sci 1990, 15, 629.
10. Duplay, C.; Monasse, B.; Haudin, J. M.; Costa, J. L. Polym Int 1999, 48, 320.
11. Lellinger, D.; Floudas, G.; Alig, I. Polymer 2003, 44, 5759.
12. Jerschow, P.; Janeschitz-kriegl, H. Int Polym Proc 1997, XII, 72.
13. Brydson, J. A. Plastics Materials, 6th ed.; Butterworth-Heinemann: London, 1995.
14. Gregoriou, V. G.; Kandilioti, G.; Bollas, S. T. Polymer 2005, 46, 11340.
15. Mouzakis, D. E.; Kandilioti, G.; Elenis, A.; Gregoriou, V. G. J Macromol Sci Pure Appl Chem 2006, 43, 259.
16. Mlynarcikova, Z.; Kaempfer, D.; Thomann, R.; Mulhaupt, R.; Borsig, E.; Marcincin, A. Polym Adv Technol 2005, 16, 362.
17. Pucciariello, R.; Villani, V.; Guadagno, L.; Vittoria, V. Polym Eng Sci 2006, 46, 1433.
18. Chrissafis, K.; Paraskevopoulos, K. M.; Stavrev, S. Y.; Docoslis, A.; Vassiliou, A.; Bikiaris, D. N. Thermochim Acta 2007, 465, 6.
19. Golebiewski, J.; Galeski, A. Comp Sci Tech 2007, 67, 3442.
20. Pogodina, N. V.; Winter, H. H.; Srinivas, S. J Polym Sci Polym Phys Ed 1999, 37, 3512.
21. Koscher, E.; Fulchiron, R. Polymer 2002, 43, 6931.
22. Kennedy, M.; Brown, G. R.; St-Pierre, L. E. Polym Compos 1984, 5, 307.
23. Supaphol, P.; Spruiell, J. E. J Appl Polym Sci 2000, 75, 44.